

Fluorescence Mapping and Photobleaching of Dye-Labeled Latex Particles Dispersed in Poly(vinyl alcohol) Matrices with a Near-Field Optical Microscope

M. Rücker,[†] P. Vanoppen,[†] F. C. De Schryver,^{*,†} J. J. Ter Horst,[†] J. Hotta,[‡] and H. Masuhara[‡]

Department of Chemistry, University of Leuven, Celestijnenlaan 200F, B-3001 Heverlee-Leuven, Belgium, and Department of Applied Physics, Osaka University, Yamadaoka, Suita, Osaka 565, Japan

Received May 26, 1995; Revised Manuscript Received July 24, 1995*

ABSTRACT: Polymer composite films consisting of fluorescent nanometric dye-labeled latex particles dispersed in poly(vinyl alcohol) matrices were imaged with a near-field scanning optical microscope (NSOM). Films with a thickness of $\sim 10\ \mu\text{m}$ and of $\sim 25\ \text{nm}$ containing latex particles with a diameter of $103 \pm 9\ \text{nm}$ with low particle density were studied. During image acquisition with the NSOM the particles were excited by an argon ion laser at the maximum or at the red edge of the excitation band at the excitation wavelength, λ , of $\lambda = 458\ \text{nm}$ or of $\lambda = 488\ \text{nm}$, respectively. Maximum fluorescence contrast occurred in the first case. Fluorescence spots with FWHM diameters of $< \lambda/2$ could be found. In the case of the $\sim 10\ \mu\text{m}$ thick films particles could only be imaged by mapping their fluorescence if they were located at the polymer-air interface. Subinterface particles could be detected as well. Additionally, photobleaching of a single fluorescent latex particle with a NSOM was performed, demonstrating a controlled photochemical reaction on a submicrometer length scale.

I. Introduction

To an increasing extent near-field scanning optical microscopy¹ is employed for studying heterogeneous organic systems by mapping their optical and photophysical properties. Concerning fluorescence mapping with a near-field scanning optical microscope (NSOM),^{2,3} certain fluorescent organic dyes became a matter of investigation because of their readily addressable excitation and their strong fluorescence. The high photosensitivity of current NSOM permits us to read out and to spectroscopically analyze fluorescence light emitted from single dye molecules.⁴⁻⁸ However, less effort has been expended in using fluorescence mapping with a NSOM for the structural investigation of organic films.⁹ In general, an addressable dye fluorescence can be applied as a probe in order to induce a defined fluorescence contrast in organic multicomponent systems exhibiting low optical contrast by selectively labeling or staining one component with a fluorescent dye. This method^{10,11} has been applied to fluorescence microscopy of heterogeneous polymer systems¹² and has been extended to laser confocal fluorescence microscopy of colloids¹³ and of polymer blends.¹⁴ However, the lateral resolution of these far-field optical techniques is diffraction-limited to approximately $\lambda/2$ of the employed excitation wavelength, λ , by the use of conventional irradiation and detection optics. Moreover, the depth resolution of these techniques ranges at best near the micrometer regime, lacking the possibility to locate the depth of fluorescence sites precisely. Concerning resolution capability, near-field optical microscopy is superior to these techniques.¹⁵

On the one hand this paper describes the structural investigation of fluorescent, heterogeneous polymer films with a NSOM operated for fluorescence detection.

These films consist of coumarin-labeled latex particles randomly dispersed in a poly(vinyl alcohol) (PVA) matrix. They resemble films of a completely phase-separated two-component polymer blend, in which one phase is enriched with coumarin. Moreover, due to their known morphology, mechanical and photochemical stability, and defined spectral property, these films represent one of the best test samples for fluorescence mapping with a NSOM. Other groups¹⁶⁻¹⁹ have already demonstrated fluorescence contrast obtained with a NSOM by imaging dye-labeled latex beads, but using different films with different beads. On the other hand this paper addresses the issue of optical near-field induced photochemistry in small spatial domains. The photobleaching of a single fluorescent latex particle with a NSOM is demonstrated, representing a specifically addressed photochemical reaction.

The employed NSOM comprises an optical and an electromechanical function unit. The optical unit is used to irradiate locally a sample under investigation by means of glass fiber optics and to detect the radiation emanating from the sample in reflection or in transmission by means of far-field optics. The irradiation is performed by coupling the light of an argon ion laser via a glass fiber coupler into a single-mode optical fiber. The opposite end of this fiber is coupled to a NSOM aperture probe. The probe is the central element of the NSOM because its properties primarily determine the attainable image resolution.¹⁵ It is fabricated by pulling a pointlike heated single-mode glass fiber past the breaking point. Afterward, the produced tapered end is coated with an aluminum film in such a way that a small aperture with a diameter of several 10 nm is left free at the break point. If light is properly coupled into the opposite end, then it propagates along the fiber and it is transmitted through the aperture. It generates a collimated radiation field in the range of approximately 5–20 nm behind the aperture. If a sample is brought to a distance of around 10 nm toward the aperture, then merely a small sample volume is efficiently irradiated. The characteristic dimension of this volume is smaller

* To whom correspondence should be addressed.

[†] University of Leuven.

[‡] Osaka University.

Abstract published in *Advance ACS Abstracts*, October 1, 1995.

than the wavelength of the coupled light, enabling subwavelength resolution in reading out fluorescent properties of the studied sample. The distance regulation of the probe toward the sample is carried out within the electromechanical function unit by a method called shear force feedback.^{20,21} In order to set this feedback, an oscillator is employed which excites a resonance oscillation of the probe tip parallel to the sample surface by a piezoceramic element. This oscillation is monitored by a laser diode shining light onto the probe tip, and a photodiode detecting the intensity modulation of the laser diode light. Finally, a lock-in amplifier phase-sensitively determines the amplitude or the phase of the photodiode signal. Both values are a function of the shear force acting on the probe. Since the shear force in turn is a function of the distance between probe and sample, this distance can be maintained approximately constant by maintaining the amplitude or the phase of the resonance oscillation constant by applying appropriate control electronics. Thus a topography image can be acquired when the sample is scanned by a piezoceramic positioner in a preslected area beneath the probe. In addition, and this is the special feature of a NSOM, an optical image can be simultaneously acquired by detecting with far-field optics in reflection or in transmission the light which emanates from the sample carrying information about fluorescent properties.

II. Experimental Section

The studied polymer composite films were prepared from dilute solutions of a latex particle solution (Poly-Sciences, type 16662) and PVA ($M_w = 88k$) with distilled water. The latex particle solution consists of carboxylate microspheres dissolved in deionized water with 2.5 wt % solids latex. The particles were produced by emulsion polymerization²² of styrene, yielding particles with a nominal diameter of 103 ± 9 nm. Finally, a coumarin dye with a maximum excitation and emission at 458 nm and at 540 nm, respectively, was attached to the particle surface enveloping the polystyrene.²³ Two different polymer films were studied. A ~ 10 μm thick film was prepared by solvent casting an aqueous solution containing 0.0001 wt % solids latex and 1 wt % PVA onto a 1 mm thick glass slide. Additionally, a ~ 25 nm thin film was produced by spin-coating an aqueous solution of 0.01 wt % solids latex and of 1 wt % PVA onto a 200 μm thick microscope coverslip. The spin-coating conditions were critical. Rotation speeds of 50 rpm for the initial 5 s and 2000 rpm for the following 60 s were set. The thickness of the PVA matrix was determined with a profilometer (Sloan Dektak3). Prior to fluorescence mapping with the NSOM, the films were characterized by measuring the excitation and emission spectra with a spectrofluorometer (Spex Fluorolog 1691) and by taking fluorescence micrographs.

The corresponding spectra obtained from a thin film are displayed in Figure 1. Qualitatively, the latex particle solutions mixed for the film preparation and the thin and thick films prepared on glass substrates provide the same excitation and emission spectra. On the basis of these spectra, it is possible to determine the excitation wavelength for maximum fluorescence intensity and to select appropriate optical filters for suppressing the excitation light without substantially reducing the intensity of the fluorescence light. The vertical arrows in Figure 1 denote two different wavelengths being used for fluorescence excitation with the NSOM. The fluorescence micrographs (not shown here)

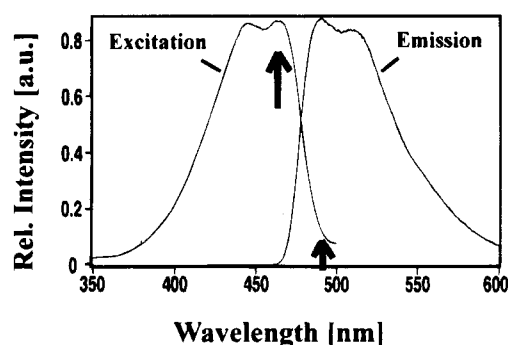


Figure 1. Excitation and emission spectrum of a ~ 25 nm thin polymer film consisting of coumarin-labeled latex particles embedded in a PVA matrix. The left and the right arrows placed in the excitation band denote the excitation wavelength, λ , of $\lambda = 458$ nm and of $\lambda = 488$ nm, respectively, used for fluorescence excitation during different NSOM experiments.

were taken with an inverted microscope (Nikon Diaphot TMD 35) in epifluorescence mode at an excitation wavelength band of 430–450 nm using a dichroic mirror as a cutoff filter. It allowed the detection of fluorescence light in the spectral range of 527–550 nm. These micrographs depict distinct fluorescence sites with high density.

For the NSOM studies an Aurora instrument and aperture probes with a nominal aperture diameter of 50 nm from Topometrix were used. The instrument was coupled via a single-mode optical fiber (3M, type FS-SN 3224) to a power-stabilized multiple-line argon ion laser (Spectra Physics, model 2025-5) serving as an external light source. The polymer films were selectively irradiated with an excitation wavelength, λ , of $\lambda = 458$ nm or of $\lambda = 488$ nm, while the NSOM was operated in illumination mode.¹⁷ The power passing the probe aperture was measured to be typically 0.5 nW in the far-field. The superimposed forward scattered excitation and generated fluorescence light were collected in the transmission mode by an objective (Nikon $\times 60$, NA 0.7), separated from the forward scattered excitation light by a long-pass color filter (Schott, OG 515, 3 mm), and focused through a pinhole onto the photocathode of a photomultiplier tube (PMT; Hamamatsu, R4632p). In addition, residual stray light of the laser diode with the wavelength of 670 nm was blocked with band-pass color filters (Schott, BG 18, 4 mm). The probe was resonantly oscillated parallel to the polymer–air interface with the smallest possible amplitude which still guaranteed an accurate distance control. The relative distance between probe and sample was maintained approximately constant by controlling the phase of the probe oscillation to correspond to a preset value. During image acquisition the preset scan speed ranged from 15 to 30 ms per image element.

Prebleaching of a thin polymer film was performed with radiation produced by a mercury discharge lamp. In order to prevent photodegradation of the polymer film, the radiation was limited to the spectral range of $\lambda > 360$ nm by the use of a long-pass color filter (Schott, GG 375, 3 mm). The film was irradiated over a time span of 16 h with a power flux of 9 mW/cm².

III. Results and Discussion

Figure 2 shows three sets of NSOM images taken one after the other from the same section of a thin polymer film. The left and the right image of each set represent the topography and the optical image, respectively, which were simultaneously acquired by applying shear

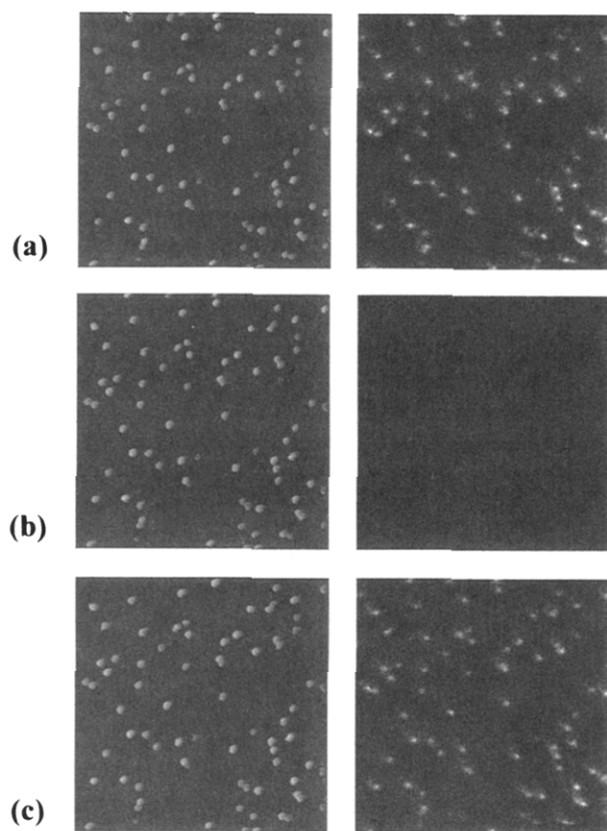


Figure 2. Three NSOM image sets successively taken from the same section of a ~ 25 nm thin polymer film consisting of coumarin-labeled latex particles embedded in a PVA matrix. Each image set (a), (b), and (c) comprises the topography image (left) and the fluorescence map (right) of this section. Image sizes: $10 \times 10 \mu\text{m}^2$. The black-white contrast in the topography images corresponds to 161 nm. The signal-to-background ratio in the fluorescence maps amounts to 2.5. The image sets (a), (b), and (c) were acquired while the polymer film was irradiated through the aperture probe at the excitation wavelength, λ , of $\lambda = 458$ nm, $\lambda = 488$ nm, and $\lambda = 458$ nm, respectively. The power output of the argon ion laser was matched to provide a light intensity of 0.5 nW at each wavelength behind the probe aperture in the far-field.

force feedback and by mapping the fluorescence light, respectively. The optical image is referred to hereafter as a fluorescence map. The uppermost image set (a) was acquired while irradiating the film through the aperture probe with the excitation wavelength of $\lambda = 458$ nm. That corresponds to maximum coumarin excitation according to Figure 1. The beadlike structures in the topography images can be attributed due to their measured sizes to single latex particles. The particles are not aggregated, and they are randomly distributed in the PVA matrix with low particle density that ranges from 0.6 to 1.0 particles/ μm^2 in these films.

In evaluating a larger number of topography images, structure widths and heights ranging from 350 to 500 nm and 120 to 180 nm, respectively, could be determined. These measured values are independent of the radiation power sent through the NSOM probe. On the other hand atomic force microscope (AFM) images of the thin polymer films obtained in both the contact and noncontact mode provided structure widths and heights ranging from 200 to 250 nm and 70 to 130 nm, respectively. When taking into account that the AFM probes used for imaging had radii of curvature of 20 and 50 nm and that the particles have a diameter distribution centered at 103 nm, these AFM data are in accordance with the expected polymer film morphology.

The latex particles emerge from the PVA matrix as spheres with a diameter of around 100 nm, they are partially embedded in the matrix, and they are coated with merely a thin PVA film. On the other hand the width and height values of the embedded latex particles obtained with the NSOM shear force method are both larger than the values obtained with the AFM. Since the measured width is a convolution of the width of the probe tip with the actual structure width at the polymer-air interface, it can be estimated from the measured width that the probe ends have diameters ranging from around 250 to 400 nm. The large height values, in turn, were caused by the shear force mechanism itself. Apparently, the shear force acting on the probe tip when positioned above a latex particle is stronger than when positioned above the PVA matrix. Consequently, the shear force feedback loop may retract the probe an additional distance from the latex particle in order to compensate for the stronger shear force.

Regarding the fluorescence map in Figure 2a, the particles displayed in the topography image can be correlated with distinct spots of higher fluorescence intensity than the background intensity. However, the shape of the fluorescence spots deviates from an expected disk shape. This may be due to the fact that the shape of the aperture in the aluminum coating of the tapered probe is not circular. Since the shape of the aperture affects the distribution of the radiation field overlapping with the fluorescent latex particles, it may affect the shape of the fluorescence spots as well. Having altered the excitation wavelength to 488 nm, which corresponds to an excitation at the red edge of the excitation band according to Figure 1, the centered image set (b) in Figure 2 was taken. From a comparison of the topography images of (a) and (b) it follows that both images are nearly identical, demonstrating that the latex particles were still located at their original positions. However, fluorescence spots do not appear in the fluorescence map of image set b. Obviously, the intensity of fluorescence ranged near the noise level of the optical detection system and it was too weak to be discernible on the intensity scale of the fluorescence map of (a). In order to assure that no modifications of the experimental conditions like, e.g., enlargement of the probe aperture or photobleaching of the coumarin dye have taken place during NSOM operation and to account for the loss of fluorescence in (b), the first experiment was repeated. The lowermost image set (c) in Figure 2 was acquired, while the film was again illuminated with an excitation wavelength of 458 nm. A comparison of image sets a and c yields that the topography image and the fluorescence map of set c reproduce the data of set a with high accuracy. Hence, this implies that the low fluorescence intensity exhibited in the fluorescence map of image set b was indeed due to an inefficient fluorescence excitation. Additionally, the almost identical topography images depicted in Figure 2 demonstrate that this polymer film can be reproducibly imaged without damaging the polymer-air interface by applying the shear force method. Moreover, this experiment shows that fluorescence of single latex particles can be specifically excited with the NSOM by tuning the excitation wavelength into the excitation band of the fluorescent coumarin dye. On the other hand the optical detection system of the NSOM is sensitive enough in order to map this fluorescence. Even when the centers of two neighboring particles are separated by a distance of less than 300 nm, these

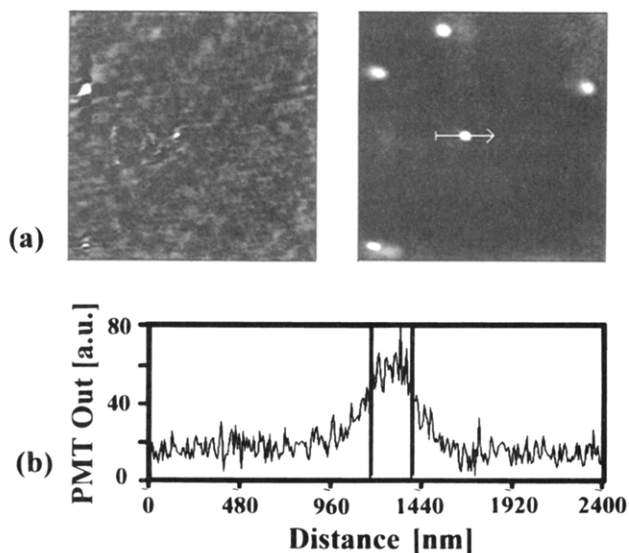


Figure 3. (a) NSOM image set comprising a topography image (left) and a fluorescence map (right). This image set displays a section of a $\sim 10\text{ }\mu\text{m}$ thick polymer film which consists of coumarin-labeled latex particles embedded in a PVA matrix. During image acquisition the polymer film was irradiated with an excitation wavelength of 458 nm. Image sizes: $10 \times 10\text{ }\mu\text{m}^2$. The black-white contrast of the topography image corresponds to 8 nm. The signal-to-background ratio of the fluorescence map data amounts to 5. (b) Profile of fluorescence intensity along the indicated arrow in the fluorescence map. The two vertical lines denote the positions of half-maximum fluorescence intensity. The full width at half-maximum amounts to $\sim 210\text{ nm}$.

particles can be spotted in the fluorescence maps as single particles. This finding demonstrates that sub-wavelength resolution in mapping fluorescence of the thin polymer composite films can be achieved.

The same experimental scheme was successfully repeated with a $\sim 10\text{ }\mu\text{m}$ thick polymer film. Figure 3 shows one image set representing on the left side the topography and on the right side the fluorescence map. Both images were simultaneously taken from the same film section at an excitation wavelength of 458 nm. At this excitation maximum, fluorescence spots of high light intensity appear in the fluorescence maps, and they can be attributed to fluorescence of these sites. Some of these spots clearly correlate with interface structures exhibited in the topography image. The height of these structures amounts to less than 8 nm. This is much smaller than the diameter of a latex particle. Consequently, in evaluating the topography image, it cannot unambiguously be concluded that these structures represent latex particles. However, by correlating the topography image with the fluorescence map, the particles can be spotted by their fluorescence which is revealed in the maps. Thus, the protrusions in the topography image at the sites of the fluorescence spots can be explained by latex particles which are located at the polymer-air interface and which emerge at best slightly from the embedding PVA matrix. Remarkably, the latex particles accounting for the uppermost centered and the uppermost right fluorescence spot in Figure 3a can hardly be seen in the topography image. In this case the particles seem to be hidden in the PVA matrix. However, these subinterface particles can unambiguously be detected by mapping their fluorescence. This finding reveals a unique capability of a NSOM. In contrast to most scanning probe microscopes, a NSOM is able to probe subinterface properties occurring in spatial domains that are located

a few 10 nm beneath a sample-air interface. The luminescence properties of these domains can be addressed by the collimated radiation field generated by the aperture probe. In addition, the interpretation that we merely excite and detect latex particles in the vicinity of the polymer-air interface is sustained by fluorescence microscopy micrographs (not shown here) which we have taken from the same type of polymer films. In these micrographs many more fluorescence spots per unit area are revealed than in the corresponding fluorescence maps taken with the NSOM. This is due to the fact that the used fluorescence microscope images all fluorescent particles located in the complete volume beneath a selected field of view. The number of particles situated at the immediate polymer-air interface, however, is much smaller than the number of particles embedded in the film volume.

The diameter of the fluorescence spots in the fluorescence map of Figure 3a is significantly smaller than the wavelength of the excitation light. Figure 3b displays the profile of a cut along the marked line in the fluorescence map of Figure 3a. The determined full width at half-maximum (FWHM) of the spot diameter amounts to $\sim 210\text{ nm}$, which is smaller than half of both the excitation and observation wavelengths. Referring to the attainable resolution in mapping fluorescent latex particles, this experiment implies that two neighboring fluorescence spots may be resolved as single spots if their centers are separated from each other by a distance of more than 210 nm. By using probes with smaller apertures, even smaller FWHM spot diameters could be observed in the maps.

Having investigated the photophysical properties of the polymer films in terms of their fluorescence, we turned to the addressing of their photochemical properties in terms of photobleaching a single latex particle with the NSOM. The coumarin dye applied for tagging the latex particles is very stable with respect to oxidation and photochemical degradation. Even after storing the polymer films under ambient conditions over a period of several months, fluorescence of the coumarin-labeled latex particles could still be observed without a detectable loss of intensity. Additionally, the irradiation of the latex particles with the NSOM probe during repeated scanning of a larger section as, e.g., the one depicted in Figure 2, did not photobleach the particles within the detection limit of the instrument either. These findings show that the tendency of the coumarin dye to photobleach is indeed very small. First experiments concerning local photobleaching controlled by the NSOM probe revealed that with a radiation power of 0.5 nW which was applied for fluorescence mapping, irradiation periods of several hours were required for attaining a detectable photobleaching. Two experimental schemes seemed to be promising in order to facilitate photobleaching via irradiation with the NSOM probe in terms of reducing the irradiation period for complete photobleaching: On the one hand an increase of the radiation power transmitted through the probe aperture results in a larger photon flux impinging on the coumarin molecules. This increases the probability for photobleaching and, finally, reduces the required irradiation period. However, a large radiation power transmitted through the NSOM probe can considerably heat up and subsequently destroy the opaque aluminum layer, forming the aperture at the probe tip. This may result in a probe with an ill-defined aperture and presumably with poor resolution capabilities. On the

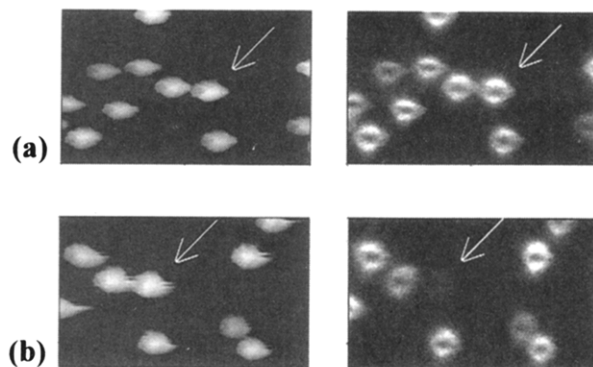


Figure 4. (a) NSOM image set comprising the topography image (left) and the fluorescence map (right) of a section of a ~ 25 nm thin polymer film. Prior to fluorescence mapping, the film was prebleached (see text for details). (b) NSOM image set consisting of a topography image (left) and a fluorescence map (right) taken from almost the same film section displayed in (a) after photobleaching the denoted particle with a NSOM probe. Both sections, however, are partially shifted with respect to each other. Light of the wavelength of 458 nm, a NSOM probe with a relatively large aperture, and a power throughput of ~ 2 nW measured in the far-field were employed for photobleaching as well as for mapping fluorescence. The arrows in (a) and (b) denote the latex particle selected for photobleaching and the corresponding fluorescence structures in the topography images and in the maps, respectively. Image sizes: $3.9 \times 2.5 \mu\text{m}^2$. The black–white contrast of the topography images corresponds to 175 nm. The signal-to-background ratio of the fluorescence map data amounts to 3.3.

other hand a reduction of the number of fluorescent coumarin molecules on the latex particles by prebleaching with an external light source reduces the number of photons required for complete photobleaching of a single latex particle with the probe. This strategy dispenses with the high radiation power transmitted through the aperture probe.

We followed the second scheme by prebleaching a thin polymer film. This was accomplished by illuminating the film ex-situ with an external mercury lamp over a period of 16 h. Figure 4a shows a section of such a prebleached thin polymer film that was used for the photobleaching experiment. For the fluorescence mapping as well as for the photobleaching of a selected latex particle a NSOM probe with a relatively large aperture diameter and a power throughput of ~ 2 nW measured in the far-field was used. All latex particles occurring in the topography image of Figure 4a clearly correlate with fluorescence structures in the corresponding fluorescence map. Interestingly, these fluorescence structures have a torus-like shape in contrast to the disk-shaped fluorescence spots displayed in Figure 2a–c and Figure 3a, and they merely occurred when using probes with rather large instead of small apertures. Probably, they do not directly reflect the dye distribution on the particles, but they result from the overlap of the individual intensity distribution of the radiation field beneath the aperture with the isotropic distribution of the coumarin molecules within a latex particle. If the radiation pattern in the plane of the polymer–air interface is torus-shaped, then a fluorescent particle images this radiation pattern, resulting in a torus-shaped structure in the fluorescence map. In the course of the photobleaching experiment, the NSOM probe was positioned above the particle denoted with an arrow in the topography image of Figure 4a, and the particle was raster-scanned while the particle was irradiated with the 458 nm light emanating from the probe. Raster-scanning was carried out in order to ensure that the

entire particle was exposed. After the particle was irradiated over a time period of 2 h, the image set displayed in Figure 4b was acquired. In strong contrast to the fluorescence map of Figure 4a, almost no fluorescence emerges from the denoted position in the fluorescence map of Figure 4b, where the probe illuminated the latex particle. However, the topography image of Figure 4b exhibits that the particle was not removed during scanning and remained at its original position. This means that indeed the majority of the coumarin molecules attached to the selected latex particle underwent a photochemical decomposition in terms of photobleaching which accounts for the loss of fluorescence. Thus it was demonstrated that a photochemical reaction can be induced upon irradiation with the NSOM probe. Moreover, further information about the properties of the photobleaching process can be deduced from the image sets in Figure 4. Although the photobleached particle is located at a distance of merely 590 nm from the next neighboring one, the latter seemed not to have been essentially affected by the 2 h of long irradiation of the photobleached particle. This implies that, predominantly, the photobleached particle was exposed to the laterally restricted radiation field of the optical near-field. Consequently, it can be concluded that the photochemical reaction induced by the optical near-field was restricted to a submicrometer length scale. In addition, the latex particle selected for extended irradiation occurs in the topography images of Figure 4a,b with essentially the same shape, indicating that the polystyrene forming the latex particle was not photochemically degraded. This means that the photobleaching of the coumarin dye was specifically addressed with the NSOM probe without inducing photodegradation of the latex particle.

In general, the presented photobleaching of a dye-labeled latex particle illustrates the possibility of specifically modifying appropriate interfaces with a NSOM. It is an example of manipulating interfaces in-situ in a controlled way on a submicrometer length scale with a submicroscopic probe.

IV. Conclusions

We have used a NSOM in order to locally excite and to map the fluorescence of labeled composite polymer films at excitation wavelengths of 458 or 488 nm. These kinds of polymer films consist of coumarin-labeled latex particles with a diameter of 103 ± 9 nm formed by polystyrene which is dispersed in a PVA matrix of known thickness with low particle density. On the one hand these polymer films can be used as test samples due to their rather defined morphology for demonstrating the capabilities of a NSOM concerning fluorescence mapping. On the other hand a polymer film of the presented type can be regarded as a model system for a film of an immiscible polystyrene and PVA blend in which both components are completely phase-separated and in which polystyrene was stained with a dye in order to provide fluorescence contrast. We report that stained polystyrene particles can be imaged by mapping their fluorescence even when hidden in a PVA matrix. This illustrates a unique capability of a NSOM operated for fluorescence detection, namely, that subinterface particles can be detected. The particle fluorescence can be read out with a lateral resolution of better than $\lambda/2$, which represents the diffraction-limited resolution of conventional optical microscopes using far-field optics. This resolution may also be attainable with phase-

separated, real polymer blends offering promising prospects for the structural analysis of such systems. Concerning specific addressing of photochemical properties, we report the photobleaching of a single fluorescent latex particle resulting from photodegradation of fluorescent coumarin molecules induced by the optical near-field emanating from a NSOM probe. This photobleaching is specifically addressed to the coumarin dye because the polystyrene forming the latex particle was not photodegraded upon irradiation. Moreover, this photochemical reaction was performed at the polymer-air interface on a submicrometer length scale demonstrating near-field induced interface machining that is accessible by a NSOM. Consequently, near-field scanning optical microscopy represents a promising avenue not only to the performance of photochemistry in small spatial domains but also to the monitoring of induced photochemical reactions.

Acknowledgment. The authors thank Keiji Sasaki for his valuable advice in sample preparation and Mark Van der Auweraer for fruitful discussions. The authors thank DWTC for financial support through IUAP-II-16 and IUAP-III-040. H.M. acknowledges partial support by a Grant-in-Aid on Priority-area Research "Photoreaction dynamics" from the Ministry of Education, Science, and Culture, Japan (06239101). J.H. is a Research Fellow of the Japanese Society for the Promotion of Science.

References and Notes

- (1) For an introduction see, e.g.: Pohl, D. W. *Adv. Opt. Electron. Microsc.* **1991**, *12*, 243. Betzig, E.; Trautman, J. K. *Science* **1992**, *257*, 189. Courjon, D.; Bainier, C. *Rep. Prog. Phys.* **1994**, *57*, 989. *Near Field Optics*; Pohl, D. W., Courjon, D. Eds.; NATO ASI Series, Series E 242; Kluwer: Dordrecht, The Netherlands, 1993.
- (2) Betzig, E.; Lewis, A.; Harootunian, A.; Isaacson, M.; Kratschmer, E. *Biophys. J.* **1986**, *49*, 269.
- (3) Fischer, U. Ch. *J. Opt. Soc. Am.* **1986**, *B3*, 1239.
- (4) Betzig, E.; Chichester, R. J. *Science* **1993**, *262*, 1422.
- (5) Ambrose, W. P.; Goodwin, P. M.; Martin, J. C.; Keller, R. A. *Phys. Rev. Lett.* **1994**, *72*, 160.
- (6) Trautman, J. K.; Macklin, J. J.; Brus, L. E.; Betzig, E. *Nature* **1994**, *369*, 40.
- (7) Xie, X. S.; Dunn, R. C. *Science* **1994**, *265*, 361.
- (8) Ambrose, W. P.; Goodwin, P. M.; Marin, J. C.; Keller, R. A. *Science* **1994**, *265*, 364.
- (9) Moers, M. H. P.; Gaub, H. E.; Van Hulst, N. F. *Langmuir* **1994**, *10*, 2774.
- (10) Billingham, N. C.; Calvert, P. D. *Dev. Polym. Charact.* **1982**, *3*, 229.
- (11) *Photophysical and Photochemical Tools in Polymer Science*; Winnik, M. A., Ed.; NATO ASI Series, Series C 182; Reidel Publishing Co.: Dordrecht, The Netherlands, 1986.
- (12) Calvert, P. D.; Ryan, T. G. *Polymer* **1978**, *19*, 611. Calvert, P. D.; Ryan, T. G. *Polymer* **1984**, *25*, 921. Billingham, N. C.; Calvert, P. D.; Uzuner, A. *Polymer* **1990**, *31*, 258.
- (13) Sasaki, K.; Koshioka, M.; Masuhara, H. *J. Appl. Spectrosc.* **1991**, *45*, 1041.
- (14) Li, L.; Sosnowski, S.; Chaffey, C. E.; Balke, S. T.; Winnik, M. A. *Langmuir* **1994**, *10*, 2495.
- (15) Betzig, E.; Trautman, J. K.; Harris, T. D.; Weiner, J. S.; Kostelak, R. L. *Science* **1992**, *251*, 1468.
- (16) Osazaki, S.; Sasatani, H.; Hatano, H.; Hayashi, T.; Nakamura, T. *Mikrochim. Acta* **1988**, *III*, 87.
- (17) Trautman, J. K.; Betzig, E.; Weiner, J. S.; DiGiovanni, D. J.; Harris, T. D.; Hellman, F.; Gyorgy, E. M. *J. Appl. Phys.* **1992**, *71*, 4659.
- (18) Fujihira, M.; Monobe, H.; Muramatsu, H.; Ataka, T. *Ultramicroscopy* **1995**, *57*, 118.
- (19) Moers, M. H. P.; Van Hulst, N. F.; Ruiter, A. G. T.; Bolger, B. *Ultramicroscopy* **1995**, *57*, 298.
- (20) Toledo-Crow, R.; Yang, P. C.; Chen, Y.; Vaez-Iravani, M. *Appl. Phys. Lett.* **1992**, *60*, 2957.
- (21) Betzig, E.; Finn, P. L.; Weiner, J. S. *Appl. Phys. Lett.* **1992**, *60*, 2484.
- (22) *Emulsion Polymerization*; Piirma, I., Ed.; Academic Press, New York, 1982.
- (23) PolySciences, Inc., the manufacturer of the coumarin-labeled carboxylate microspheres, noted that the coumarin molecules are attached to the surface of the microspheres.

MA9507249